Steel and Composite Structures, *Vol. 30, No. 4* (*2019*) *383-392*
DOI: https://doi.org/10.12989/scs.2019.30.4.383

Improving the hysteretic behavior of Concentrically Braced Frame (CBF) by a proposed shear damper

Ali Ghamari [1], Hadi Haeri [*2], Alireza Khaloo [1] and Zheming Zhu [2]

[1] *Department of Civil Engineering, Sharif University of Technology, Tehran, Iran*
[2] *MOE Key Laboratory of Deep Underground Science and Engineering, School of Architecture and Environment, Sichuan University, Chengdu 610065, China*

(*Received October 13, 2018, Revised February 10, 2019, Accepted February 23, 2019*)

Abstract. Passive steel dampers have shown favorable performance in last earthquakes, numerical and experimental studies. Although steel dampers are more affordable than other types of damper, they are not economically justified for ordinary buildings. Therefore, in this paper, an innovative steel damper with shear yielding mechanism is introduced, which is easy to fabricate also can be easily replaced after sever earthquakes. The main goal of implementing such a mechanism is to control the possible damage in the damper and to ensure the elastic behavior of other structural components. The numerical results indicate an enhancement of the hysteretic behavior of the concentrically braced frames utilizing the proposed damper. The proposed damper change brittle behavior of brace due to buckling to ductile behavior due to shear yielding in proposed damper. The necessary relations for the design of this damper have been presented. In addition, a model has been presented to estimate load-displacement of the damper without needing to finite element modeling.

Keywords: passive steel dampers; stiffness; ductility; seismic behavior

1. Introduction

During Northridge (1994) and Kobe (1995) earthquakes, while many buildings had been designed to withstand the tremors and thus save human lives, a large number of steel buildings suffered severe damage and lost their structural functions. After the mentioned earthquakes, important experimental and numerical studies on beam-to-column connections were developed in the USA and Japan, including the works on Reduced Beam Section (RBS) (Zarei *et al*. 2016, Lu *et al*. 2018a, Zahrai *et al*. 2017a, Akrami and Erfani 2015) the cover plate or haunch. Two types of plate reinforced connections had been studied: the cover-plate and the flange-plate connection (Lu *et al*. 2018b, Averseng *et al*. 2017), no weld access hole by Kim (Kim and Oh 2007) and improved weld access hole (Suita *et al*. 1998).

Although these improved connections had shown satisfactory performance in experimental studies, the seismic design of these details were based on the plastic rotation capacity of the main frame (beam and column). Thereby, when these details are used, the damaged buildings cannot be easily repaired (Oh *et al*. 2009). Since, after an earthquake, it is important to quickly restore the buildings and their pertinent functions in the affected urban areas, these welded connection details would not be effective options when the severity and the damages of recent disasters are considered.

To overcome these types of problems, the use of passive energy dissipation devices for the control of damage in structures has previously been proposed (Lee and Kim 2015).

Passive energy dissipation systems have been considered as effective and inexpensive means of mitigating earthquake risks to structures. The passive energy dampers that promote the functionality of structures are considered as an advanced and effective technology in structural engineering. By improving these devices, the design of structures is directed towards the reduction and dissipation of seismic energy by increasing the structural ductility and the damping capacity. Structural stability under seismic loads, and the quick repair or replacement of some structural elements after an earthquake are some of the important advantages of using energy dampers. In addition to the desirable dynamic performance of a system in resisting the applied loads, the ease of implementation is another important issue that must be considered to guarantee a satisfactorily functioning system. On the other hand, economical considerations and architectural aspects must also be taken into account. The main reason for using passive energy dissipation devices in a structure is to limit the damages in structural components.

Among the available varieties of passive energy dissipation devices, the metallic-hysteretic damper is one of the most effective and economical mechanisms for the dissipation of seismic energy input, which is achieved through the inelastic deformation of metallic material.

Numerous metallic dampers (devices) have been developed to be installed between beams and columns in a frame structure (Vatansever and Kutsal 2018, Ma *et al*.

*Corresponding author, Ph.D., E-mail: haerihadi@gmail.com

Copyright © 2019 Techno-Press, Ltd.
http://www.techno-press.org/?journal=scs&subpage=6
ISSN: 1229-9367 (Print), 1598-6233 (Online)

2011, Koetake *et al*. 2005). These devices mainly used to improves of Concentrically Braced Frames (CBFs).

The CBF systems have a high elastic stiffness and strength against lateral loading. The stiffness and strength of the CBF is decreased due to buckling of compression diagonal member under cyclic loading and the degradation is revealed in hysteresis curves of in compression zone (Suita *et al*. 1998).

Therefore, by degradation of the stiffness and strength in nonlinear behavior under cyclic loading, the capability of energy absorption of CBF system will significantly have decreased. By reduction of slenderness, the hysteresis curve of CBF system is improved. Although hysteresis is improved, degradation of energy absorption (due to compression member) is not omitted completely. It is due to inherent of buckling in compression member. So, despite of good elastic stiffness and ultimate strength of the CBF system, due to low capability in energy dissipation, it have introduced as an inadequate system under seismic loading. Numerous metallic dampers have been proposed to improve the hysteretic behavior of the CBF systems: TADAS (Mahmodi and Abdi 2012), ADAS (Khazaei 2013, Zhu *et al*. 2018), the Buckling-Restrained Brace (BRB) which changes the buckling behavior of conventionally braced frame to yield under both tension and compression without significant buckling (Sabelli *et al*. 2003, Tremblay *et al*. 2006, Lu *et al*. 2018c), and the slit damper (Eldin *et al*. 2018, Shahri and Mousavi 2018, Lee and Kim 2015, 2017). These devices have been mainly designed to be incorporated into the bracing system of structural frames. Rai (Rai *et al*. 2013) developed an idea of using shear dampers made of steel and aluminum with low yield points.

Among of presented damper until now, the shear damper has a better performance than others ones.

Generally, the shear damper are more commercial than BRB systems and more easily for fabrication than ADAS and TADAS. Shear damper attached to CBF system has investigated by Bouwkamp *et al*. (2016), Vetr *et al*. (2017), Vetr and Ghamari (2019) numerically and experimentally. In the studies, shear damper has installed between braces and floor beam that reduces elastic stiffens.

In the present paper an innovative shear damper is introduced, which is easy to fabricate and install and can be easily replaced after strong earthquakes. This proposed damper changes the brittle behavior (buckling) of diagonal brace system to ductile behavior (yielding). The proposed damper, as mentioned earlier, is easy to build and can be fabricated and installed readily at the construction site, in omparison with the famous dampers such as: ADAS, TADAS, viscous dampers, friction dampers, and BRB, which are being presently utilized worldwide. The proposed damper is more economical than the mentioned dampers. As explained in the text, the simple proposed device is first installed on the diagonal bracing member while still on the ground, and then installed on the structure. Therefore, the proposed system does not require stringent supervision since, for instance, overhead and vertical welds are omitted.

2. The proposed damper

2.1 Damper geometry

The proposed damper consists of four plates, which are inscribed by a cylinder. The steps for making the damper are shown in Fig. 1. The damper, illustrated in Fig. 1, is uncomplicated for fabrication and installing. It can be easily created and attached to structure without the help of skilled technicians. For creating and fabricating the damper, it only need a primary technicians that is a considerable advantage for the damper**.**

Fig. 2 shows schematic views of the geometry and placement of the proposed damper. For simplicity, the damper has been shown for a two-story single bay frame; but it can be used in multi-story structures. This damper can be fabricated out of shop and under proper supervision. In addition, since overhead and vertical welds are not required, the welds will have a high quality. After fabricating the damper, it can be easily attached to the diagonal element by welding or friction bolts. It should be noted that gusset plate in the proposed system and CBF system are the same. Moreover, rigid or simple connection can be utilized for connection between beam to column.

2.2 Design criteria

In all obtained relations as well as the numerical models, a hinge type connection has been assumed between beams

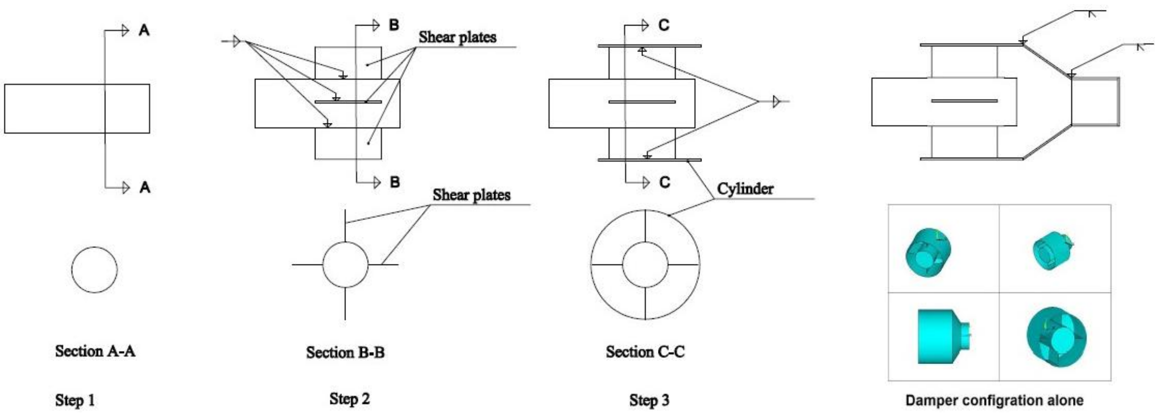

Fig. 1 Fabrication of the proposed damper

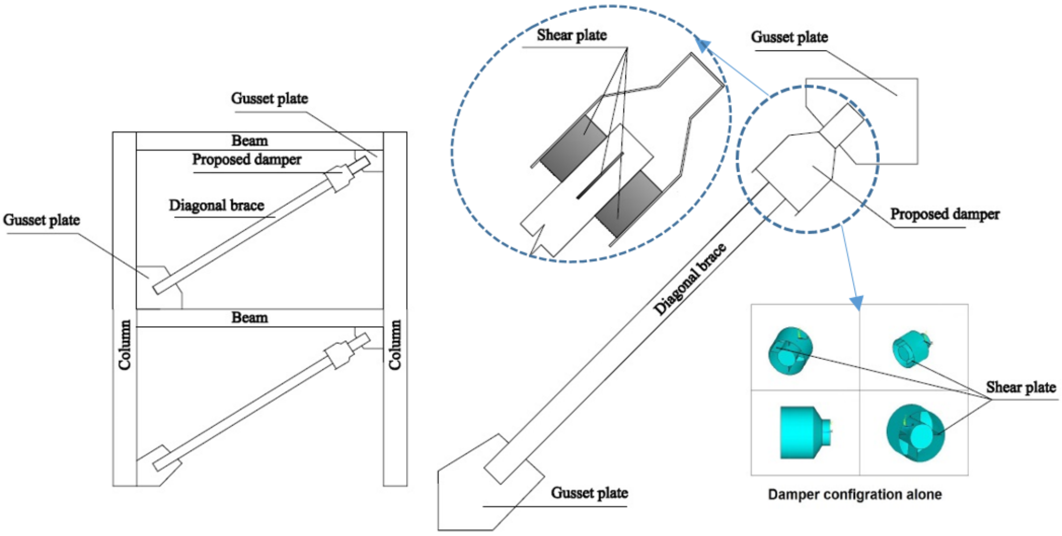

Fig. 2 Schematic views and placement of the damper in frame

and columns. Therefore, the developed relations have exclusively concentrated on the diagonal bracing element and the proposed damper. If connection between beam to columns be hinge, all lateral load is carried by brace (with or without damper). In this state, proposed relations are used directly to analysis or design of the system. If connection between beam to columns be rigid, interaction of moment frame and brace element (with or without damper) should be accounted. To take into account of the interaction, lateral load is divided between moment frame and brace (with or without damper) according to their stiffness. After dividing lateral load between moment frame and brace, system is designed based on the existing relations. So, relations to calculate stiffness, strength brace frame (with damper) is proposed in the next sections.

2.2.1 Stiffness

The manner of placement and connection of damper to the structural member results in a series combination of the equivalent springs of diagonal brace stiffness and damper stiffness; which the diagonal axial stiffness and shear stiffness of damper plates (along the diagonal axis) provide the equivalent shear stiffness of the system (refer to Fig. 3).

Hence, the equivalent spring of system's stiffness can be calculated from the fundamental relations of structural analysis, as follows

$$\frac{1}{K_e} = \frac{1}{K_b} + \frac{1}{K_d} \tag{1}$$

In this relation, K_b and K_d are the brace stiffness and damper stiffness, respectively, which can be determined as

$$K_b = \frac{E.A}{L}, K_d = \frac{G.A_d}{d} \tag{2}$$

where the E, G, A and A_d is elasticity modulus, shear modulus, cross section area of the brace, cross section area of the plates of damper. In addition, L and d has shown in Fig. 4.

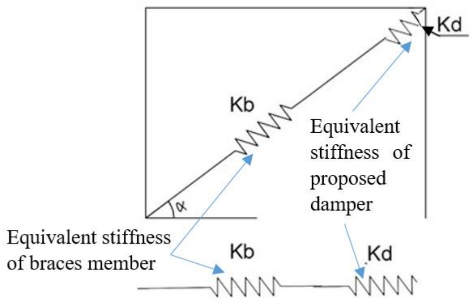

Fig. 3 Simplification of model to determine the stiffness

With the introduction of parameter β as

$$K_e = \frac{\beta}{1+\beta} K_b = \gamma K_b \tag{3}$$

The equivalent stiffness (along the diagonal brace member axis) of damper and diagonal element will be defined as a factor of the diagonal element stiffness. Thus

$$\beta = \frac{K_d}{K_b} \tag{4}$$

Therefore, the closer the factor γ $(\gamma = \frac{\beta}{1+\beta})$ approaches to one, the more the system stiffness will converge to diagonal stiffness.

The displacement of the plates of shear damper is limited according to story drift to prevent the failure of plates of shear damper. The limitation for each frame are quantified by considering a lower bound value at displacements corresponding to 2.5% drift for the frame.

3.2.2 Strength

In seismic design, in addition to the stiffness criterion, the strength and ductility criteria are also highly important. The configuration of the shear damper and the diagonal brace member must be such that the shear yielding of the

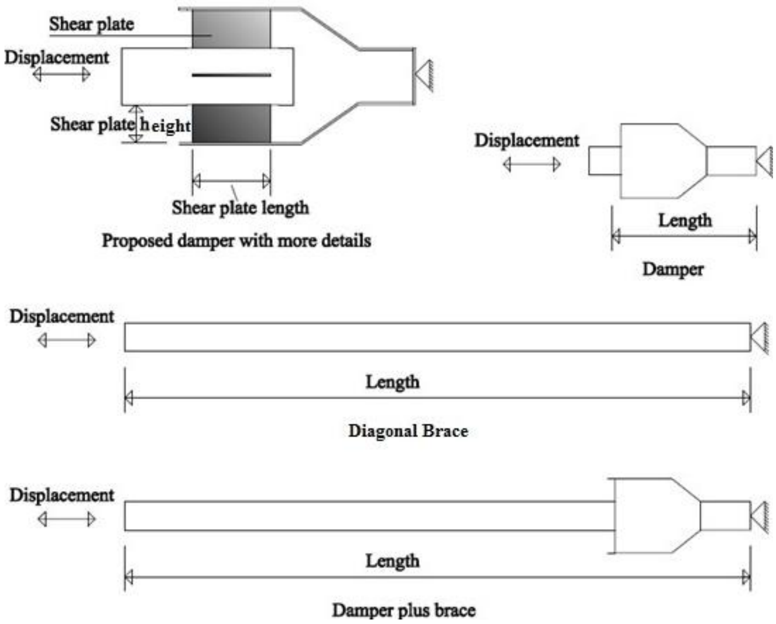

Fig. 4 System definitions

damper is the governing mode of system behavior. Eventually, this component should be designed in such a way that it can withstand large inelastic deformations without losing strength. Based on AISC-341, without accounting strain hardening effect, the damper's maximum plastic shear will be equal to

$$\mathrm{V_p} = 0.6 A_d F_{yd} \tag{5}$$

The design strength for flexural buckling of compression members is $\emptyset P_n$, where P_n nominal resistance in compression is

$$P_n = \left(0.658^{\lambda_c{}^2}\right) F_y . A \qquad For\ \lambda_c \leq 1.5 \tag{6}$$

$$P_n = \left(\frac{0.877}{\lambda_c{}^2}\right) F_y . A \qquad For\ \lambda_c \leq 1.5 \tag{7}$$

Where

$$\lambda_c = \frac{KL}{r\pi}\sqrt{\frac{F_y}{E}} \tag{8}$$

Where λ_c is the slenderness parameter, A is the gross cross-sectional area, Fy is the specified minimum yield stress, E is the modulus of elasticity, K is the effective length factor, L is the unbraced member length in the plane of buckling, and r is the radius of gyration of the cross-section about the axis of buckling. Eq. (6) is the design strength for inelastic buckling and the Eq. (7) is the design strength for elastic buckling. The slenderness parameter $\lambda_c = 1.5$ is the slenderness parameter that demarcates between inelastic behavior from elastic behavior.

The critical elastic buckling stress F_e is determined as follows

$$F_e = \frac{\pi^2 E}{\lambda^2} \tag{9}$$

To ensure that the shear yielding of proposed damper occurs before buckling of brace member, the below relation should be applied

$$\mathrm{V_p} \leq \emptyset P_n \tag{10}$$

The applicability of the above relation and the system's ductile performance can be guaranteed by limiting the slenderness, λ. The results of these calculations by means of plastic analysis principles and the compliance with AISC requirements are proposed below in the form of a simple relation.

$$\begin{cases} \lambda \leq 1.54\pi\sqrt{\dfrac{E}{F_y} Ln(0.6\dfrac{A_d}{A} \times \dfrac{F_{yd}}{F_y})} \\ \lambda \leq 1.21\,\pi\sqrt{\dfrac{E}{F_y} \times \dfrac{A}{A_d}} \end{cases} \tag{11}$$

where the F_y, F_{yd} stress yielding of brace and stress yielding of plates of shear damper, respectively. Other parameters were defined in section 3.3.1

The above relation will be correct, if Ln is positive. Therefore, the following relation needs to be satisfied.

$$\frac{A_d}{F_{yd}} < 1.67\frac{A}{F_y} \tag{12}$$

3. Numerical studies

3.1 Study procedure

The proposed damper was studied from various aspects so that comprehensive findings on its behavior can be presented. In order to confirm the accuracy and calibration of the relations presented in Section 2 of this paper and to investigate the overall performance of the shear damper, first, several damper models were analyzed by just changing the thickness of the plates of shear damper. The results of these analyses were used in designing the interaction between the shear damper and the bracing system. In this regard, full-scale models were simulated and analyzed under cyclic loads. In these examples, the desired results were extracted by altering the slenderness of the brace and keeping the properties of the proposed damper constant.

Table 1 Specifications of FE modeling

Model name	Type of model	Length (mm)	Plate thickness (mm)	Plate length (mm)	Plate height (mm)
t6	Damper	--	6	150	75
t4	Damper	--	4	150	75
t2.67	Damper	--	2.67	150	75
t2	Damper	--	2	150	75
L30	Damper	--	4	300	75
L23	Damper	--	4	230	75
L18	Damper	--	4	190	75
L12	Damper	--	4	112	75
L7.5	Damper	--	4	75	75
H25	Damper	--	4	15	25
L415	Brace only	4150	--	--	--
L480	Brace only	4800	--	--	--
L536	Brace only	5360	--	--	--
L587	Brace only	5870	--	--	--
DL339	Damper+ brace	3040	15	150	100
DL415	Damper+ brace	3800	15	150	100
DL480	Damper+ brace	4450	15	150	100
DL536	Damper+ brace	5010	15	150	100
DL587	Damper+ brace	5520	15	150	100

3.2 Geometrical specifications

In Table 1, the numerical models and their specifications have been listed. In sample model names, letter "t" indicates the sole damper, "L" indicates the sole brace and "D" represents the complete system (consisting of the diagonal element and the damper attached to it). Damper length is 35 cm and the length of plates of shear damper is 15 cm. The rest of the geometrical specifications have been given in Table 1.

3.3 Material properties

The shear damper and the compressive bracing members have been made out of structural steel ST37 with a yield stress of 240 MPa, and the cylindrical protection sheath around the plates of shear damper has been made out of hard steel with a rupture stress of 520 MPa.

3.4 Numerical modeling

The nonlinear analysis of the Finite Element (FE) method program by ANSYS software was utilized to investigate the proposed damper. All elements were modeled by SHELL element with 4-nodes and 6 degree of freedom. After several trial and error experiments, the optimum FE mesh sizing was selected. Fig. 5 shows a schematic of meshing of the FE modes.

Mesh formation has been such that at common points, structural nodes are established and coupled with each other using the capability of the software. It should be noted that the mesh formation has also been checked by the capability of the software.

To perform a geometrical and material nonlinear analysis and also to consider imperfections, a technique in the nonlinear FE modeling in ANSYS software has been implemented. In doing so, first, an elastic buckling analysis was carried out and after evaluating the buckling modes; the dominant mode was introduced to the software. By this technique, the imperfection is counted.

For evaluating the convergence of the results, two force and moment convergence criteria were employed. The isotropic hardening have been utilized for behavior of materials.

In the local modeling of the shear damper, the "t4" model was chosen as the reference model and then the plate

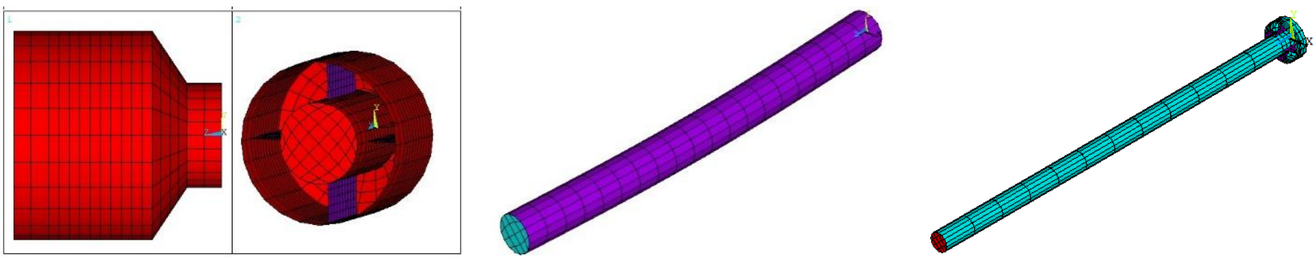

(a) (b) (c)

Fig. 5 FE models: (a) Damper only; (b) Brace only; (c) Damper attached to brace

Table 2 Specifications of proposed damper models

Model	t (mm)	$\frac{t}{t_{model\ t4}}$	λ	$\frac{\lambda}{\lambda_{model\ t4}}$
t6	6	1.5	25	0.67
t4	4	1	37.5	1
t2.67	2.67	0.65	57.69	1.54
t2	2	0.5	75	2

Table 3 Specifications of brace models

Model	Length (mm)	Slenderness λ	$\frac{\lambda}{\lambda_{model\ L480}}$	P_{cr} (N)	$\frac{P_y}{P_{cr}}$
L415	4150	80.42	0.86	588.15	0.75
L480	4800	93.01	1	439.64	1.00
L536	5360	103.86	1.12	352.58	1.25
L587	5870	113.75	1.22	293.97	1.50

thickness (and aspect ratio, λ) of the shear damper (t in Table 2) was increased or decreased. Increasing "t" increases aspect ratio, λ. Other needed specifications have been presented in Fig. 4 and Table 2.

In the comparison of braces, tube section with outside diameter of 150 mm and thickness of 4 mm has been used. Considering the identical cross sections of braces, the yield force is equal to 440 kN. In these samples, with the change of length, different magnitudes of buckling force (P_{cr}) and yield force (P_y) have been obtained, which are shown in Table 3. In these models, the L480 sample has been selected as the reference sample.

3.5 Loading

Cyclic loading has been applied based on the control of displacement. For this purpose, first, an analysis has been performed to determine the yield point displacement (Δy), and then the displacement has been increased [increased or decreased] by $\mp\Delta_y, \mp 2\Delta_y, \ldots$..

4. Estimation and analysis of results

4.1 Validation of FE results

An experimental specimen has been selected to verify the results of FE modeling; specimen Specimen-L2SR033 from (Tanaka and Sasaki 2000). Tanaka (Tanaka and Sasaki 2000) has reported results of experimental test of some shear panels that the experimental test results are used in the paper. Fig. 6 shows the experimental test that is utilized for verification of the FE modeling. Since the proposed damper is subjected to pure shear, its behavior is exactly similar to that of the experimental shear panel. In other words, the FE modeling of the proposed damper was carried out and the numerical results were validated through comparison with the results of an experimental study. The main feature of our proposed damper is shear deformation, which is the same as

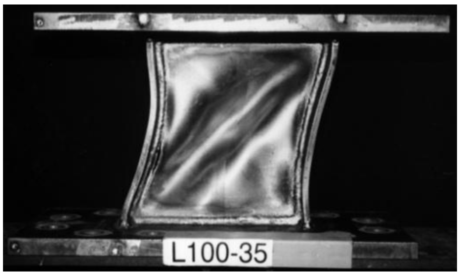

Fig. 6 Experimental test model (Tanaka and Sasaki 2000)

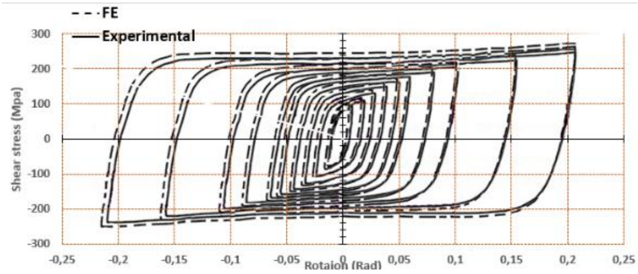

Fig. 7 Comparison between experimental and FE results

the main feature of the results of the experimental model used for verification in our study. In other words, the main feature in both studies is shear deformations. Fig. 6 shows the experimental test that is used for calibrate of the numerical models in the paper.

Fig. 7 clearly shows that the FE results obtained through ANSYS correlate very well with the experimental results. The hysteresis curves obtained from experimental test and FE modeling are in good agreement in linear and nonlinear zones. Once the results of the software are confirmed for the sample model, the other numerical models are simulated and examined to investigate the behavior of the proposed damper.

4.2 Accuracy analysis of the results

Fig. 8 illustrates the results of nonlinear analysis under cyclic loading. It can be seen, the shear damper has stable, reliable, and full hysteresis curves. Under cyclic loads, the damper can absorb energy, without any loss of strength, until the point of rupture; therefore, it can be relied upon as a deformation fuse with ductile behavior. The important point is that, after yielding, the strength of the damper increases. Although this is considered an advantage, it should be taken into account in the designing of connections and brace elements. The damper can bear up to 7 times the deformation corresponding to yielding; thus, its ductility can be considered equal to 7. In addition, the shear strength of the plate, depending on its thickness, has increased to 1.1 to 1.25 times the strength corresponding to yield strength, which is due to strain hardening under shear. Of course, many researchers have maintained that steel structures under shear yielding are able to withstand loads that are even higher than 1.25 times the yield strength.

Comparison of the ultimate hysteresis curves (maximum loop) of damper in Fig. 9 shows that the increase of plate

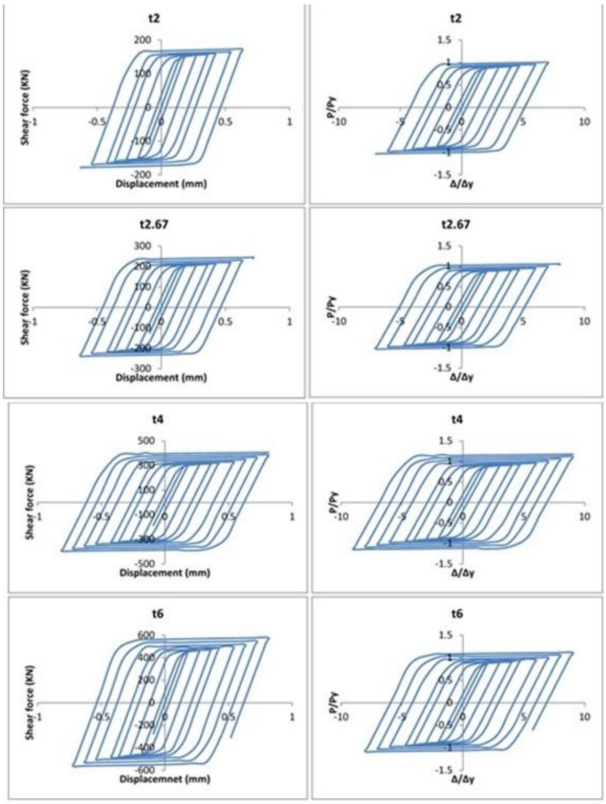

Fig. 8 Hysteresis curves of damper

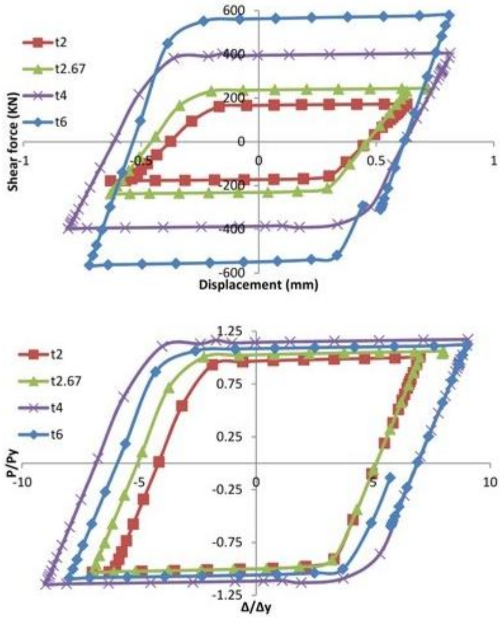

Fig. 9 Comparing the maximum hysteresis curves of samples

thickness leads to the increase of shear strength and its energy absorption capacity. In addition, by scaling the applied load to yielding capacity and scaling the applied displacement to equivalent yield displacement, it is demonstrated that plate thickness has little impact on the ductility of damper. Considering the low slenderness ratio of the plates of the shear damper, shear yielding will always

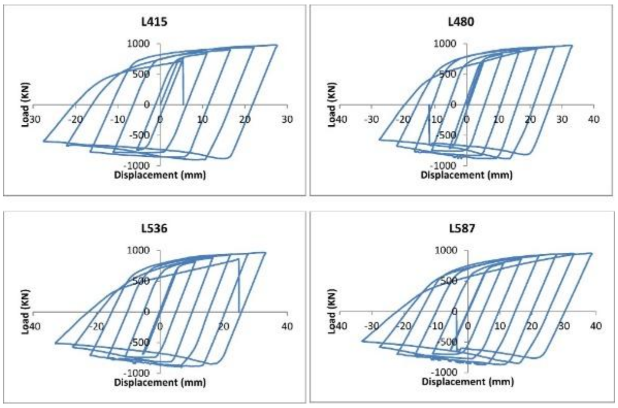

Fig. 10 Hysteresis curves of the diagonal element

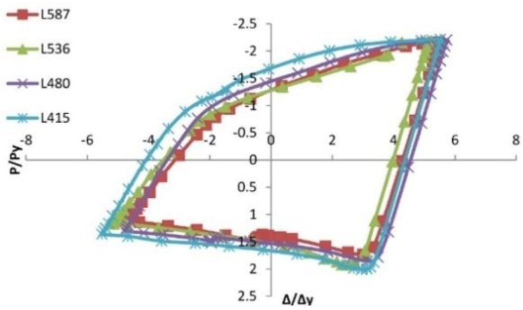

Fig. 11 Maximum loop of the diagonal element's hysteresis curve

occur prior to shear buckling.

4.3 Improving the brace behavior

The hysteresis curves of braces have been illustrated in Fig. 10, which as anticipated, show severe loss of strength in these braces under compressive loads. The degradation of brace hysteresis curve in compression is due to bucking of brace element. In Fig. 11, these curves have been normalized, and their ultimate curves display similar behaviors.

With the known hysteresis behavior of brace in Figs. 10 and 11, which indicates a loss of stiffness and strength in brace in the nonlinear phase, the proposed damper is attached to the brace and its hysteresis curves are sketched in Fig. 12. Considering of the figure shows the valuable capability of the proposed damper to enhance of the heresies curve of braces. In right of the Fig. 12, unite less hysteresis curves has been shown. In these curves, for in horizontal axial the displacement has been divided to yielding displacement and for in vertical axial the load has been divided to yielding capacity. By this technic, it can be shown that the system what the system will do after yielding. In the other words, nonlinear behavior of system is revealed.

The stable loops that have been illustrated show the changing load bearing mechanism of the brace element from compressive buckling to the shear yielding of the damper plates. In all the samples, the strength of the system increases to more than 2.5 times the yielding capacity;

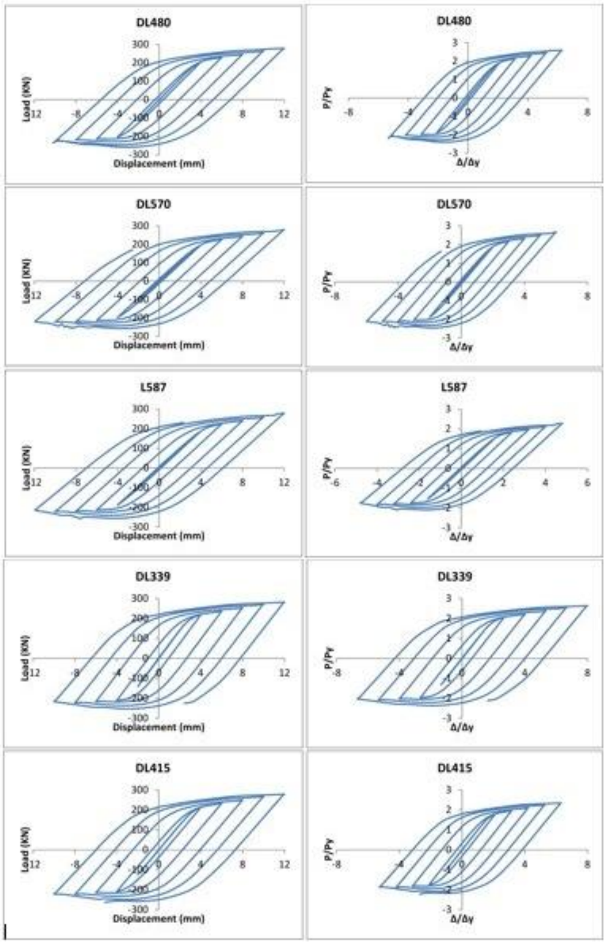

Fig. 12 Hysteresis curves of the whole system

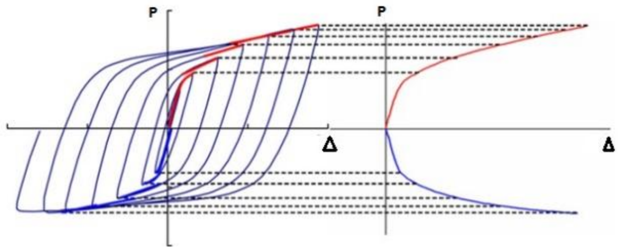

Fig. 13 Concept of skeleton curve

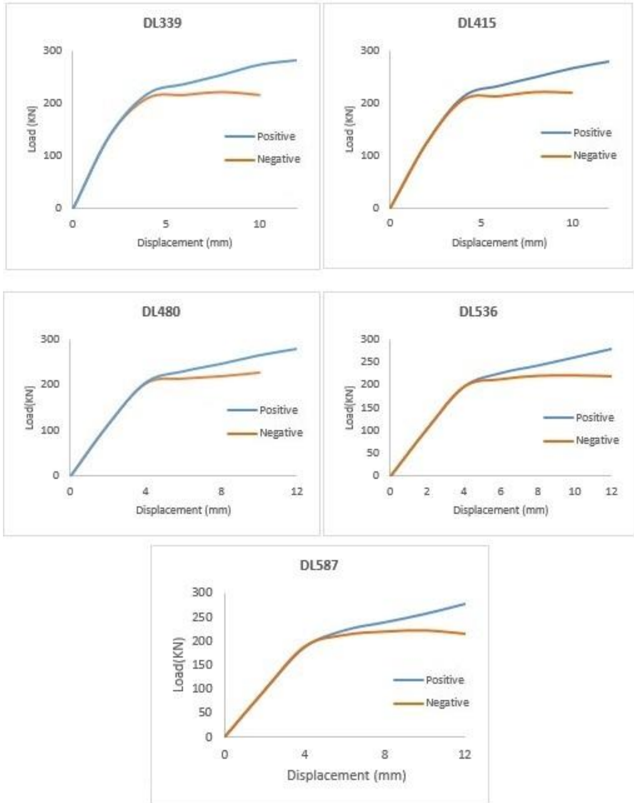

Fig. 14 Load-displacement results of Model

a behavior which is expected under compressive and tensile loads. Since the system is designed so that the yielding of the shear damper is the dominating mode of system behavior, the ultimate displacement of the system reaches 7 times the corresponding yielding displacement. In all the samples, even up to the point of yielding, the bracing element is in the elastic range, and no nonlinear behavior is observed. As described, the proposed damper improves the behavior of the convergent brace, and with the help of damper, the brittle behavior of the compressive buckling of the convergent diagonal brace leans toward the ductile behavior of the shear yielding of the proposed damper plates.

4.4 Skeleton curves

Skeleton curves are commonly adopted when characterizing the hysteretic behavior and the ductility capacity of steel members that are subjected to load reversals. It is a simplification for static analysis instead of dynamic analysis (Zhou *et al*. 2008). The concept of a skeleton curve is shown in Fig. 13. A skeleton curve is constructed by connecting skeleton portions; a skeleton portion is defined as part of a restoring force versus deformation curve that exceeds the maximum restoring force achieved in previous loading cycles.

By examining the system behavior under unidirectional loads, another aspect of system performance can be investigated. Hence, in this section, the results associated with unidirectional loads have been shown in Fig. 14. Two types of curves have been used in these diagrams so that the behaviors of the system under tension and compression can be studied separately and also by plotting these in a diagram and superimposing them on one another, the adverse effects of buckling and compressive loads can be observed. The important observation is that the elastic stiffness values of the system in tension and compression completely match and therefore, the Eq. (1) is used to estimate load displacement of system with high accuracy. The mentioned relations have been obtained based on structural analysis principles and static linear relations. The discrepancy observed in the behaviors of systems is due to their nonlinear behavior. After the structure starts to yield in tension, the strength of the system goes up and system behavior begins to improve. The rate of this strength

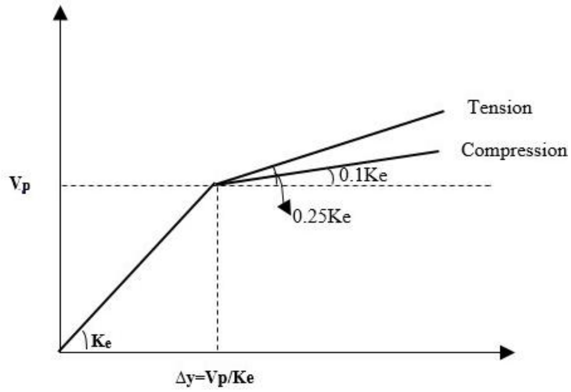

Fig. 15 Behavior of nonlinear system in tension and compression

increase will be analyzed in the following sections. However, after the onset of compression, the system will not experience a loss of strength, and an elasto-plastic behavior will be observed. This trend will be almost the same in all the samples.

4.5 Prediction of nonlinear behavior

By examining the monotonic behavior of the system, in this section, a simple method is presented for estimating the nonlinear behavior of the system. The relations presented in the previous sections can be used for designing the considered system in the elastic state, and Fig. 15 can be employed to estimate the nonlinear behavior of such a system. These curves have been calibrated by the results obtained from the numerical modeling. Therefore, by using the relations presented in the previous section, the elastic behavior of the system can be predicted and by employing the acquired curves, the system's inelastic behavior can be easily obtained.

Regarding the use of these curves, first, the equivalent stiffness and displacement of the system can be calculated by means of the relations in the previous section, and then these two data can be used to obtain the force for the onset of nonlinear behavior in the structure. After getting this point, one can refer to the graph of Fig. 15 and use the percent slopes of the tension and compression curves to separately plot the nonlinear behavior curves for the tension and compression regions and to obtain the ultimate strength of the system. After reaching this strength, the displacement increases until the system's rupture point.

5. Conclusions

In this paper, an innovative passive energy damper was introduced and its design relations were presented. This damper can be easily repaired or replaced after an earthquake and it is very easy to fabricate. To investigate the behavior of this damper, several models were analyzed and the following results were obtained:

- With the increase in the length of the diagonal members in the concentrically Braced frame, due to the increase of the slenderness ratio, compressive buckling will become the dominant mode of system behavior and the stiffness and strength degradation of the system will increase more severity. This mechanism of behavior is altered, and improved, by the use of the proposed damper.
- The use of the proposed damper transforms the brittle behavior of compressive buckling in the compressive braces into the ductile shear yielding behavior.
- Increasing of plate thickness of the proposed damper does not considerable effect on P/Py.
- By utilizing proposed damper, the ductility of CBF (that is 5.5 for CBF) is increased from 6.5 to 8. Therefore, by utilizing proposed damper, the ductility is improved from 18% to 45%.
- Since the proposed damper can be replaced after sever earthquake, it reduces cost of repairing after earthquake.
- The increase in the plate thickness of shear damper leads to the increase in the shear strength and stiffness of the damper, but it has little effect on its ductility. By increasing plate thickness, the shear strength of the shear damper can be increased up to 2 times.

References

AISC, ANSI/AISC 341-16 (2016), Seismic provisions for structural steel buildings; American Institute of Steel Construction, Chicago, IL, USA.

Akrami, V. and Erfani, S. (2015), "Effect of local web buckling on the cyclic behavior of Reduced web BeamSections (RWBS)", *Steel Compos. Struct., Int. J.*, **18**(3), 641-657.

Averseng, J., Bouchair, A. and Chateauneuf, A. (2017), "Reliability analysis of the nonlinear behaviour of stainless steel cover- plate joints", *Steel Compos. Struct., Int. J.*, **25**(1), 41-55.

Bouwkamp, J., Vetr, M.G. and Ghamari, A. (2016), "An analytical model for inelastic cyclic response of eccentrically braced frame with vertical shear link (V-EBF)", *Case Studies Struct. Eng.*, **6**, 31-44.

Eldin, M.N., Kim, J. and Kim, J. (2018), "Optimum distribution of steel slit-friction hybrid dampers based on life cycle cost", *Steel Compos. Struct., Int. J.*, **27**(5), 633-646.

FEMA (2000), Recommended seismic design criteria for new steel moment-frame buildings; In FEMA350, Washington D.C., USA.

Khazaei, M. (2013), "Investigation on dynamics nonlinear analysis of steel frames with steel dampers", *Procedia Eng.*, **54**, 401-412.

Kim, Y. and Oh, S. (2007), "Effect of the moment transfer efficiency of a beam web on deformation capacity at box column-to-beam connections", *Eng. Struct.*, **63**, 24-36.

Koetake, Y., Chusilp, P., Zhang, Z., Masakazu, A., Suita, K., Inoue, K. and Uno, N. (2005), "Mechanical property of beam-to-column moment connection with hysteretic dampers for column weak axis", *J. Eng. Struct.*, **27**,109-17.

Lee, J. and Kim, J. (2015), "Seismic performance evaluation of moment frames with slit-friction hybrid dampers", *Earthq. Struct., Int. J.*, **9**(6), 1291-3111.

Lee, J. and Kim, J. (2017), "Development of box-shaped steel slit dampers for seismic retrofit of building structures", *Eng. Struct.*,

150(1), 934-946.

Lu, L., Xu, Y., Liu J. and Lim, J. (2018a), “Cyclic performance and design recommendations of a novel weak-axis Reduced Beam Section connection”, *Steel Compos. Struct., Int. J.*, **27**(3), 337-353.

Lu, L., Xu, Y., Liu J. and Lim, J. (2018b), Cyclic response and design procedure of a weak-axis cover-plate moment connection”, *Steel Compos. Struct., Int. J.*, **26**(3), 329-345.

Lu, J., Wu, B. and Mei, Y. (2018c), “Buckling mechanism of steel core and global stability design method for fixed-end buckling-restrained braces”, *Eng. Struct.*, **174**, 447-461.

Ma, H., Jiang, W. and Cho, C. (2011), “Experimental study on two types of newbeam-to-column connections”, *Steel Compos. Struct., Int. J.*, **11**(4), 851-865.

Mahmoudi, M. and Abdi, M.G. (2012), “Evaluating response modification factors of TADAS frames”, *J. Constr. Steel Res.*, **71**, 162-170.

Oh, S., Kim, Y. and Moon, T. (2007), “Cyclic performance of existing moment connections in steel retrofitted with a reduced beam section and bottom flange reinforcements”, *Can. J. Civil Eng.*, **34**, 199-209.

Oh, S.H., Kim, Y.J. and Ryu, H.S. (2009), “Seismic performance of steel structures with slit dampers, Journal of Engineering Structures”, *J. Constr. Steel Res.*, **31**, 1997-2008.

Rai, D.C., Annam, P.K. and Pradhan, T. (2013), “Seismic testing of steel braced frames with aluminum shear yielding dampers”, *Eng. Struct.*, **46**, 737-747

Sabelli, R., Mahin, S. and Chang, C. (2003), “Seismic demands on steel braced frame buildings with buckling-restrained braces”, *J. Eng. Struct.*, **25**, 655-666.

Shahri, S.F and Mousavi, S.R. (2018), “Seismic behavior of beam-to-column connections with elliptic slit dampers”, *Steel Compos. Struct., Int. J.*, **26**(3), 289-301.

Suita, K., Nakashima, M. and Morisako, K. (1998), “Tests of welded beam-column subassemblies. II: Detailed behavior”, *J. Struct. Eng.*, **124**, 1245-52.

Tanaka, K. and Sasaki, Y. (2000), “Hysteretic Performance of Shear Panel Damper Ultra Low Yield Strength Steel for Seismic Response Control of Buildings”, *Proceedings of the 12th World Conference on Earthquake Engineering-12WCEE 2000*, Auckland, New Zealand.

Tremblay, R., Bolduc, P., Neville, R. and Devall, R. (2006), “Seismic testing and performance of buckling-restrained bracing systems”, *Can. J. Civil Eng.*, **33**, 183-198.

Vatansever, C. and Kutsal, K. (2018), “Effect of bolted splice within the plastic hinge zone on beam-to-column connection behavior”, *Steel Compos. Struct., Int. J.*, **28**(6), 767-778.

Vetr, M.G. and Ghamari, A. (2019), Experimentally and analytically study on eccentrically braced frame with vertical shear links, *Struct. Des. Tall Special Build.*, **e1587**. DOI: https://doi.org/10.1002/tal.1587

Vetr, M.G., Ghamari, A. and Bouwkamp, J. (2017), “Investigating the nonlinear behavior of Eccentrically Braced Frame with vertical shear links (V-EBF)”, *J. Build. Eng.*, **10**, 47-59.

Zahrai, S.M., Mirghaderi, S.R. and Saleh, A. (2017a), “Tubular Web Reduced Beam Section (TW-RBS) connection, a numerical and experimental study and result comparison”, *Steel Compos. Struct., Int. J.*, **23**(5), 571-583.

Zahrai, S.M., Mirghaderi, S.R. and Saleh, A. (2017b), “Increasing plastic hinge length using two pipes in a proposed web Reduced Beam Section, an experimental and numerical study”, *Steel Compos. Struct., Int. J.*, **23**(4), 571-583.

Zarei, A., Vaghefi, M. and Fiouz, A.R. (2016), “Numerical investigation seismic performance of rigid skewed Beam-to-column connection with reduced beam section”, *Struct. Eng. Mech., Int. J.*, **57**(3), 507-528.

Zhou, X.P., Zhang, Y.X. and Ha, Q.L. (2008), “Real-time computerized tomography (CT) experiments on limestone damage evolution during unloading”, *Theor. Appl. Fracture Mech.*, **50**(1), 49-56

Zhu, B., Wang, T. and Zhang, L. (2018), “Quasi-static test of assembled steel shear panel dampers with optimized shapes”, *Eng. Struct.*, **172**, 346-357.

CC